Microthrusters Employing Catalytically Reacted N_2–O_2–H_2 Gas Mixtures, Tridyne

H. E. BARBER,* G. L. FALKENSTEIN,† C. A. BUELL,‡ AND R. N. GURNITZ§
Rocketdyne, Division of North American Rockwell Corporation, Canoga Park, Calif.

An experimental program has been conducted to evaluate 10-mlb attitude-control thrusters utilizing a catalytically reactive gas (N_2-O_2-H_2) during both pulse-mode and steady-state operation. Two types of catalyst have been evaluated, and the more reactive material (Engelhard MFSA 30-mesh catalyst) has been used in a series of flightweight thrust chamber tests simulating space vacuum. The thruster pressure and temperature response characteristics are adequate to meet representative spacecraft requirements, and the thrust level is virtually constant over the reactive gas temperature range from ambient to 1500°F. Flightweight test hardware has been constructed by electrodepositing nickel over precision formed mandrels. The results of a design study are presented in which three thrusters are integrated into a typical spacecraft module. Four such modules will provide opposing thrust couples about the pitch, yaw, and roll axes. Tridyne system offers a substantial weight saving over a nitrogen cold gas system and is reasonably competitive with an advanced electrically heated gas system.

Introduction

IN the Tridyne concept, small fractions of reactive gases are combined with an inert dilutent to form a nondetonable mixture that may be safely stored at high pressure in a vessel. Energy release is accomplished by passing the mixture through a catalyst. The gas mixture for the 1500°F design operational temperature, used in Tridyne thruster tests, is 0.85 nitrogen, 0.10 hydrogen, and 0.05 oxygen by volume (or 0.9297 N_2, 0.0079 H_2, and 0.0625 O_2 by weight).

Data on Tridyne storability and the uses of various gas mixtures for pressurization were obtained on an advanced pressurization system technology program under an Air Force contract.[1] Numerous experiments with catalysts as potential ignition devices are reported under a J-2 engine ignition development program,[2] and extensive ignition experiments with O_2–H_2 propellants are documented in Ref. 3. Catalysts used with cryogenic oxygen and hydrogen propellants in reaction control systems are reported in Refs. 4 and 5.

This paper is concerned with the application of the Tridyne concept to flightweight thrusters at 0.01-lb thrust. Conventionally, simple cold-gas systems have been used in the majority of spacecraft attitude control systems of the 10-mlb class because of their inherently high reliability. Tridyne represents a modest change to this system type and provides a logical technology advancement without complex system changes. The requirements for the flightweight design established by the Jet Propulsion Laboratory are compared to the performance attained during the program in Table 1. Tridyne system weights also are compared with competitive systems[6,7] in the paper.

Experimental and Flightweight Hardware

The test configuration shown in Fig. 1a was used for the first test series in the selection of a catalyst and in the sizing of the catalyst bed. It consists of a machined, stainless-steel thrust chamber configured for assembly to a standard, flared-tube fitting, and includes provisions for varying the catalyst bed length. It was designed for flexibility in changing or modifying the catalyst bed geometry. A more nearly optimum chamber configuration was also used, which had a small, low-mass injector (Fig. 1b). In an attempt to minimize thruster heat losses, a 0.10-in. i.d. chamber (Fig. 1c), was constructed of Lavalite, a low-thermal conductivity nonmetallic composite. This chamber was found to provide the most consistent data.

The second principal design task consisted of the formulation of a three-chamber module concept for pitch, yaw, and roll control of a spacecraft (Fig. 2). Two opposing chambers are oriented for pitch and yaw control in a vertical plane with a roll chamber at a right angle to the vertical chambers. The thrusters are configured for ease of assembly into a thermally efficient, three-chamber cluster and heater module. The concept provided a basis for a realistic flightweight thruster configuration and for a determination of the probable thruster heat loss rates that would occur in a spacecraft installation.

A flightweight thruster design was established based on the module thrusters. As shown in Fig. 2, the chamber body is a cylindrical section with an injector and screen at the inlet to

Table 1 Performance comparison

	Specified value	Program value
Vacuum thrust (calculated), lb	0.01 ± 0.002	0.01 ± 0.0004
Expansion, ϵ	100:1	100:1
Chamber pressure P_c range, psia	15–30	30 selected
Impulse bit (calculated), lb-sec $\times 10^4$	2.4 ± 0.4	2.0 ± 0.2
Valve excitation time, msec	20	20
Thrust response time, msec		
From signal to 0.02 $P_{c_{max}}$	6	6
From signal to 0.9 $P_{c_{max}}$	8	8
Nominal pulse width	20	20
Thrust decay times, msec		
Off signal to 0.1 $P_{c_{max}}$	8	8

Presented as Paper 70-614 at the AIAA 6th Propulsion Joint Specialist Conference, San Diego, Calif., June 15–19, 1970; submitted July 9, 1970; revision received September 28, 1970. The work reported herein was conducted under technical direction of the Jet Propulsion Laboratory, Pasadena, Calif., Contract NAS 7-719.

* Member of Technical Staff. Member AIAA.
† Manager, Small Engines Analysis. Member AIAA.
‡ Member of Technical Staff.
§ Manager, Exploratory Engineering.

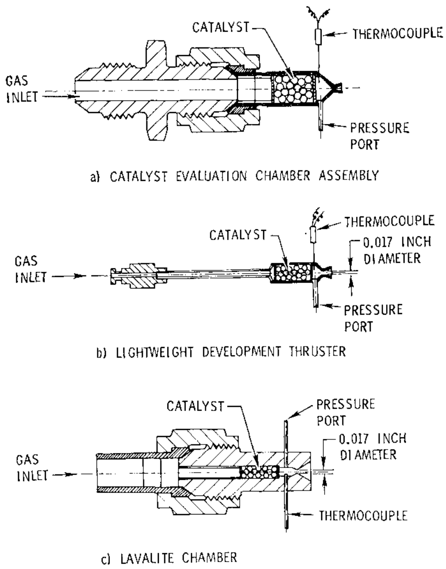

Fig. 1 Experimental hardware.

provide a uniform distribution of Tridyne through the catalyst bed. The catalyst bed also has a screen at the downstream face, which is positioned 40° from the chamber axis. The screen is elliptical in shape and configured to match the chamber and nozzle section truncations. The exit nozzle and throat section is formed by joining two cones (nozzle section with 16° half-angle and convergent section with 33° half-angle) by a wall radius three times the throat radius.

The convergent section is cut at a complementary angle (50° from the nozzle centerline) to form an elliptical face matching the chamber section. Using this design approach, the chamber is easily constructed by electrodepositing nickel over two simple mandrels with a screen interface. The single critical dimension is the throat diameter, which is controlled to a tolerance of ±0.0001 in.

A test configuration (Fig. 3) was assembled for evaluation of the flightweight thruster design. Difficulties were encountered in installing chamber pressure probes and chamber internal thermocouples. The best technique for installing thermocouples was found to be that of electroforming the thermocouples in place during the chamber fabrication process. Pressure probes were attached by induction brazing with high-melting point alloys.

The chamber enclosure consists of a laser beam weldment at the chamber injector interface. The weld beads are uniform and the discharge point overlap is reasonably symmetrical. The weld time per chamber was on the order of 2.5 min.

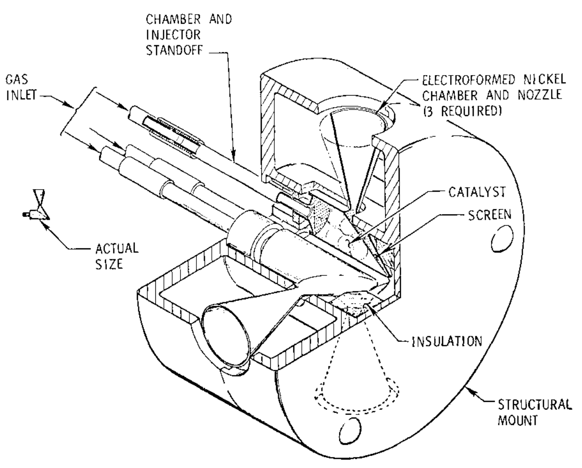

Fig. 2 Flight-type, three-engine module assembly.

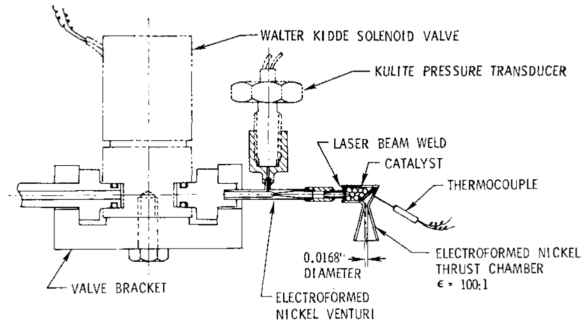

Fig. 3 Flight weight test configuration.

The thermal cycling accomplished to date on welded chambers has had no evident effect on the weld integrity. The maximum recorded chamber operational temperature was 1331°F. It was also necessary to heat the weld area to a temperature of 1700°F in assembling the test chambers to the inlet line. Here, again, no adverse effect from the heating was shown.

Experimental Results

Catalysts from Shell Development Company (Shell 405) and Engelhard Industries (MFSA) were tested in various sizes and geometrical arrangements to determine optimum catalyst quantities. Extensive tests showed that MFSA was approximately twice as responsive as Shell 405 and 30-mesh MFSA catalyst was about twice as active per unit weight as 16-mesh MFSA. For a flowrate of 1.8 sci/sec, 0.02 and 0.04 gm of 30-mesh MFSA catalyst are required at 30 and 15 psia, respectively.

Catalyst Evaluation

In previous experimental programs using $\frac{1}{16}$-in. MFSA catalyst with Tridyne at pressures up to 1000 psia, it was found that the minimum catalyst mass M'_c, required to completely react the Tridyne, could be computed by the empirical formula

$$M'_c = K\mathring{v}/P_c \tag{1}$$

where P_c = chamber pressure, psia; $\mathring{v}$ = chamber flowrate, sci/sec; and K = experimental constant for the catalyst formulation and size.

Rearranged in the form $K = M_c(P_c/\mathring{v})$ and plotting the steady-state chamber temperature as a function of $M_c(P_c/\mathring{v})$, it was found that as M_c is increased, while the flow conditions $(P_c/\mathring{v})$ were held constant, the temperature will increase to a point where all the gas is reacting. Adding more catalyst beyond this point will produce no increase in temperature. In practice, the use of excess catalyst will decrease system thermal response, and may cause a decrease in temperature, be-

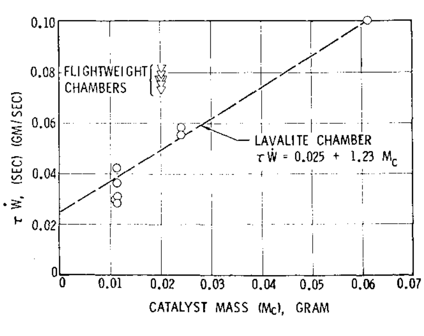

Fig. 4 Thermal time constant parameter vs catalyst mass.

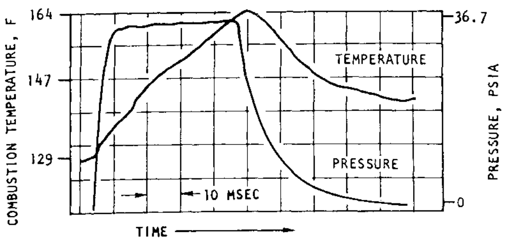

Fig. 5 Temperature and pressure response (ΔT = 35 *F/40 ms*).

cause more catalyst will be in contact with the chamber walls, thus increasing heat transfer from the gas to the chamber. A plot of the experimental results for the Lavalite chamber with 30-mesh MFSA catalyst showed that the steady-state chamber temperature T_{ss} broke sharply at $K = 0.20$; therefore, this point corresponds to the optimum amount of catalyst. Although the gas is completely reacted above $K = 0.20$, the gas temperature was measured to be below the 1500°F ideal flame temperature because of heat losses from the chamber.

If the Tridyne reaction is surface-catalyzed, and the catalyst outer surface is the effective control, then the reactivity should be proportional to the outer surface area. As the surface area per unit mass is inversely proportional to the pellet diameter, the 30-mesh catalyst has approximately twice the surface area and should exhibit twice the reactivity of the 16-mesh catalyst. The optimum K values for 30- and 16-mesh catalysts are consistent with the hypothesis.

Temperature Response Analysis

Temperature data were correlated by means of thermal time constants to facilitate configuration comparisons and to establish the temperature-time curve form for analytical performance projections. The time constant (τ) is defined as the time required for the temperature to increase from the initial value to 63% of the final steady-state temperature.

The theoretical temperature response can be estimated by means of a heat balance for the catalyst bed. The catalyst bed was assumed to be in thermal equilibrium with the gas, and the gas was assumed to react instantaneously on the catalyst's surface. If an incremental mass for the screens and chamber is included in the heat balance, the equation becomes

$$\dot{w}(-\Delta H_r)dt = \dot{w}C_p(T - T_0)dt + (M_cC_{p_c} + M_eC_{p_e})dt \quad (2)$$

where $\dot{w}$ = Tridyne flowrate, lb/sec; ΔH_r = Tridyne heat of reaction = $C_p(T_f - T_i)$, Btu/lb; M_c = catalyst mass, lb; M_e = mass due to the screens and chamber, lb; C_p = heat capacity of Tridyne, Btu/lb-°R; C_{p_c} = catalyst heat capacity Btu/lb-°R; C_{p_e} = effective heat capacity of the M_e increment, Btu/lb-°R; T = outlet temperature of Tridyne, °R, also assumed equal to catalyst bed temperature under assumption of thermal equilibrium; T_i = initial temperature of Tridyne, °R; T_f = adiabatic flame temperature of Tridyne, °R; and T_0 = initial temperature of catalyst, °R.

Integrating Eq. (2) from T_0 to T and rearranging the Tridyne outlet temperature is

$$T = T_f - (T_f - T_0)e^{-t/\tau} \quad (3)$$

where the time constant term is

$$\tau = (M_cC_{p_c} + M_eC_{p_e})/\dot{w}C_p \quad (4)$$

The equation neglects both the effects of a temperature gradient within the catalyst and heat losses. A similar heat balance can be made by considering heat losses to obtain

$$T = T_{ss} - (T_{ss} - T_0)e^{-t/\tau} \quad (5)$$

where T_{ss} is the steady-state temperature.

To investigate the validity of this analysis, the experimental value of $\tau\dot{w}$ was plotted as a function of M_c (Fig. 4) for the Lavalite chamber data. The resulting curve appears to be a linear function of catalyst mass as predicted. The intercept at $M_c = 0$ indicates that

$$M_e(C_{p_e}/C_p) = 0.025 \text{ g} \quad (6)$$

If the extra mass has the same heat capacity as the Tridyne, then M_e = 0.025 g, which is moderately less than the effective weight increment anticipated for the nickel flightweight chambers.

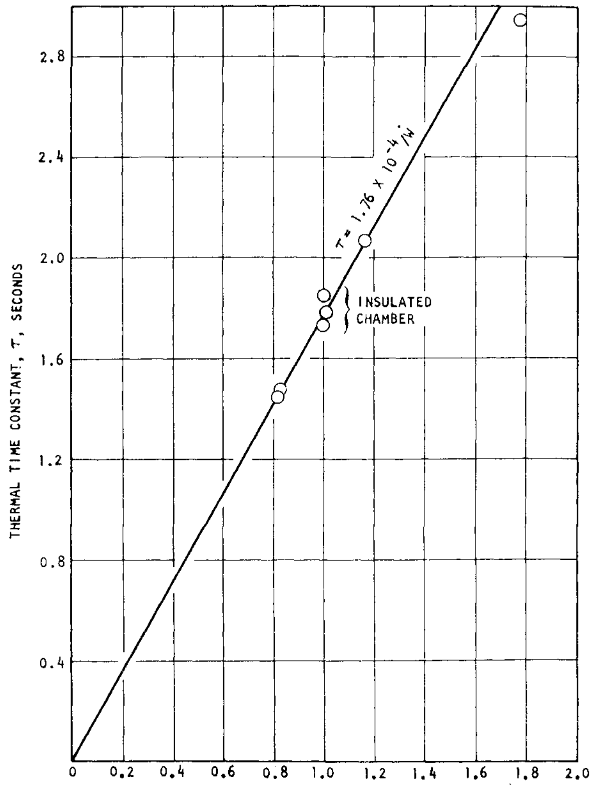

Fig. 7 The effect of flowrate on thermal time constant for the flight weight thruster.

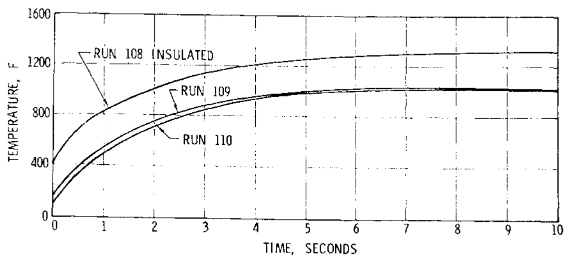

Fig. 6 Thermocouple temperature vs time (Tridyne flight weight thruster).

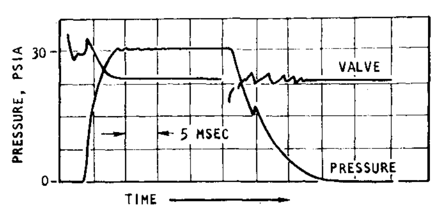

Fig. 8 Tridyne thruster 25-msec pulse.

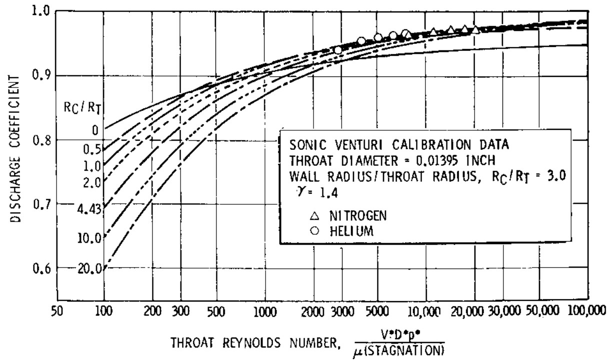

Fig. 9 Predicted values of discharge coefficient for sonic nozzles.

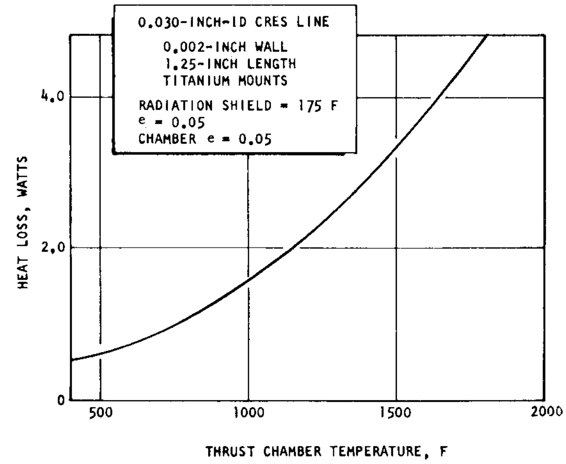

Fig. 11 Tridyne thruster module total heat loss, conduction and radiation.

Flightweight Thruster Tests

The performance characteristics of flightweight Tridyne thrusters were evaluated in both pulse-mode and steady-state operation for the optimum catalyst mass of 0.02 gm. The tests were to provide information on thermal and pressure-response characteristics and to demonstrate the feasibility of flightweight thrusters.

The test system (Fig. 3) consists of a control valve, a sonic venturi flowmeter, and a flightweight chamber. Two engine configurations were employed. One was instrumented with a thermocouple electroformed in the chamber wall; the other had a pressure probe installed in the chamber upstream of the nozzle throat. Several test runs on the former established that the thermocouple would provide excellent chamber wall temperature measurements but would not approach true gas temperature, which was computed to be approximately 1175°F for a measured chamber wall temperature of 1000°F.

A typical thermal transient is illustrated by the recorded thermocouple output (mv) during a pulse interval (Fig. 5). The temperature trace increases from 129° to 164°F during the 40-msec on-time (measured rate 875 deg/sec). The rate of decrease is also extremely fast at the pulse termination, indicating a rapid energy loss from the thermocouple juncture. Some data on the chamber thermal characteristics at high temperatures were provided during a test series to evaluate insulation effectiveness. A series of pretest checkout and instrumentation calibration firings was made that caused the chamber and inlet line to reach near equilibration at 402°F. The test was then conducted at T_i = 402°F, which increased to 1331°F at test termination. The temperature time history for the test (run 108) is shown in Fig. 6 with similar data for two subsequent tests with no insulation. As the recorded thermocouple readings were estimated to be about 175° lower than the freestream gas temperature, it was concluded that during test 108, the Tridyne closely approached the design operational temperature of 1500°F.

Six long-duration (10-sec) tests provided data for determining the thruster thermal time constant. The tests were of the type shown in Fig. 6 with the chamber initial temperature near ambient. Thermal time constants computed from the temperature response data were found to vary from 1.46 to 2.94 sec depending on the flowrate or chamber pressure.

In Eq. (4), for the thermal characterization tests, all parameters except the flowrate were constant. The time constants are plotted in Fig. 7 as a function of the flowrate. The experimental data are described by the equation $\tau = 1.76 \times 10^{-4}/\dot{w}$, which is consistent with the theoretical prediction.

To compare the thermal characteristics of the flightweight chamber with the Lavalite test configuration, the term $\tau\dot{w}$ is plotted in Fig. 4 for a catalyst mass of 0.020 g. The $\tau\dot{w}$ data for the flightweight chambers are about 50% higher than those for the Lavalite chamber. The higher time constant is attributed to an increase in the effective mass (M_e). This is possibly due to the higher effective thermal capacitance of the nickel chamber and screens in the flightweight chambers.

Pressure transient characteristics were evaluated by a fast-response Kulite transducer mounted directly on the chamber and then on the sonic venturi in the inlet line. A high degree of sensitivity to the volumes of the lines and transducer mounts was noted during these tests. By reducing the void

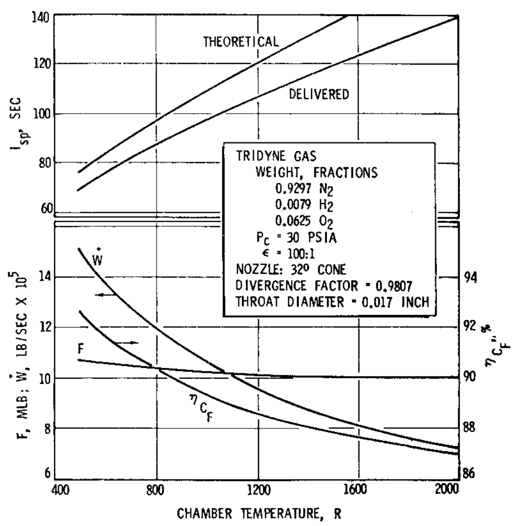

Fig. 10 Thruster parameters vs chamber temperature.

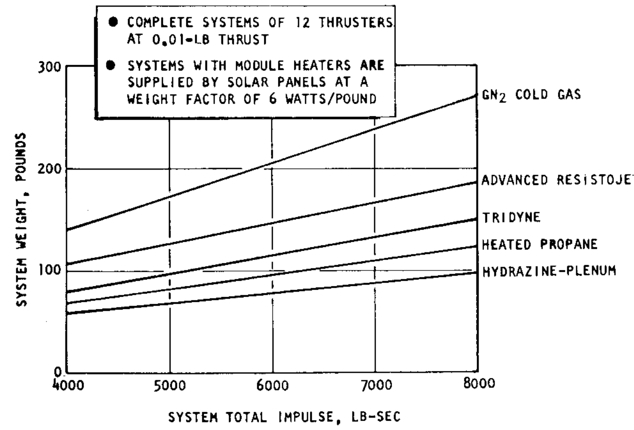

Fig. 12 System weight comparison.

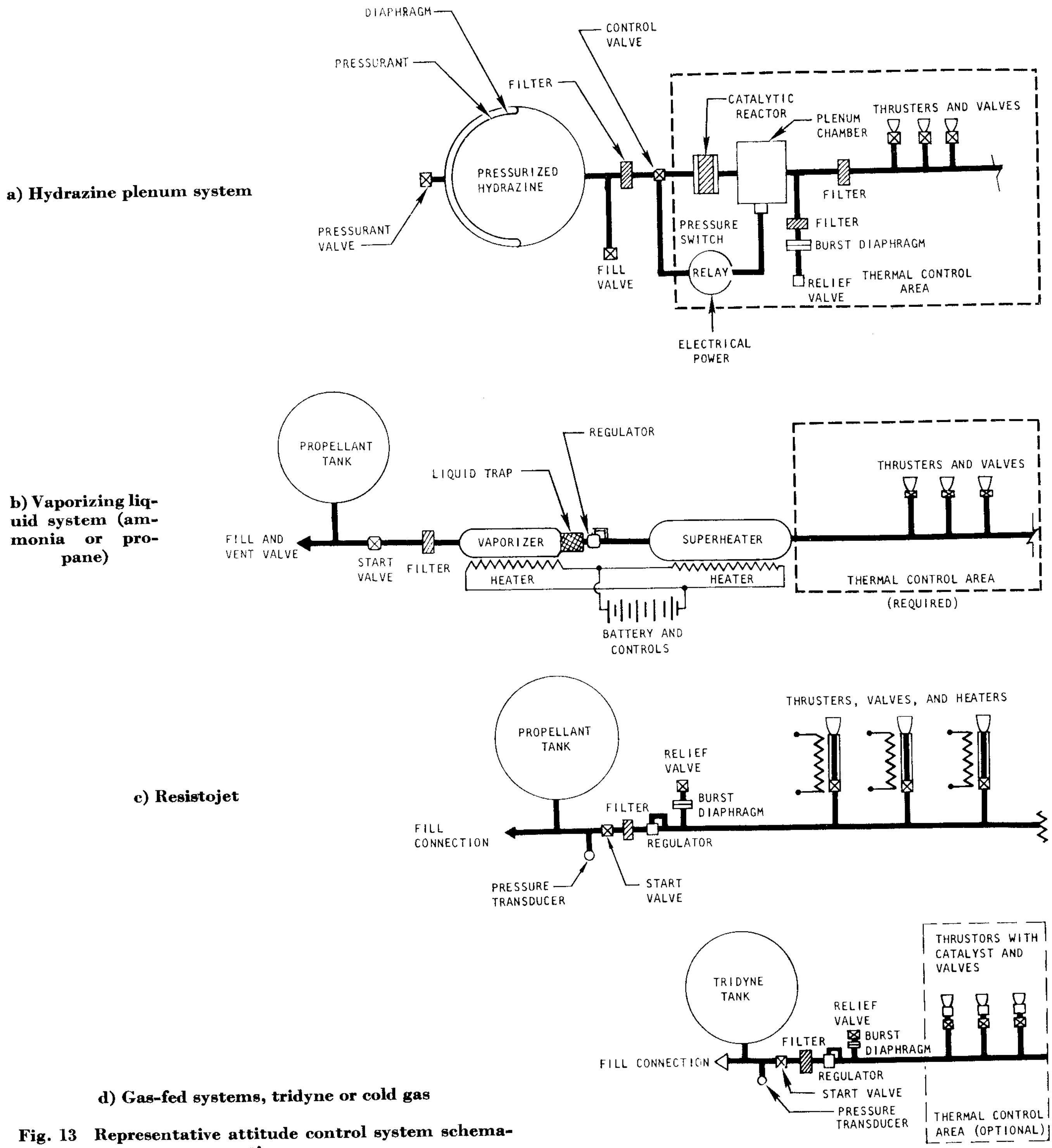

Fig. 13 Representative attitude control system schematics.

volume in the Kulite mount to a practical minimum amount, it was possible to achieve a pressure transient (Fig. 8) of 5 msec from valve open to full chamber pressure. The pressure decay time (Fig. 8) was 13 msec from the signal off to 10% of maximum pressure. A minor improvement could be effected by eliminating the instrumentation line volumes, but the program objective of 8 msec from signal off to 0.1 $P_{c_{max}}$ is probably unattainable.

Analysis

Figure 9 shows thrust chamber performance at conditions established during program development. Flow loss factors were evaluated by means of an analytical model that utilizes the integral momentum and energy equations with a finite difference solution. The loss terms—potential flow at the throat, nozzle divergence, and boundary-layer effects—are combined to determine thrust coefficient efficiency η_{CF}, which was applied to establish the delivered specific impulse. The thrust chamber effective throat area is thus determined by the flowrate required to deliver the rated thrust of 0.01 lb.

For microthrust nozzles, the boundary-layer effects are significant and substantially reduce nozzle throat effective areas. Although experimental data on discharge coefficients in the low Reynolds numbers range are somewhat limited, recent analysis of the effects of approach velocity and the boundary-layer profile has resulted in remarkably good agreement between various references. A correlation developed by Rocketdyne is shown in Fig. 9. Superposed are data acquired from calibration of the sonic venturi used for measuring thruster flowrates. Both nitrogen and helium were flowed over a pressure range of 10–50 psig, and flow vs time was measured by a Beckman positive-displacement flowmeter. The venturi throat diameter was 0.01395 in. with an error margin of less than 0.00005 in. The wall/throat radius ratio was 3:1. Calibration data show no apparent coefficient change due to the difference in specific heat ratios of helium and nitrogen (1.66 and 1.40, respectively).

The thrust F was calculated as the product of the mass flowrate $\dot{w}$ and the delivered specific impulse. The variations of $\dot{w}$ and F with temperature at a constant inlet pressure are shown in Fig. 10. It is possible that the viscous losses predicted at high temperatures by Rocketdyne's performance program are conservatively computed. The program is well substantiated at thrust levels above 1-lb thrust. However, few substantiating data are available for reference in the range of 0.01-lb thrust. This is an area warranting study and further experimental evaluating.

Module Heat Loss and Projected Performance

An important phase of the program was the projection of test data and thruster performance to conditions of spacecraft operation. The module design (Fig. 2) is the basis of the thermal analysis to establish heat loss rates from a three-chamber cluster (pitch, yaw, and roll control) and to determine heater requirements to maintain the module at a reference temperature.

A thermal analog network of the rocket engine assemblies in the three-chamber module configuration was constructed for input to the Rocketdyne Differential Equation Analyzer Program (DEAP-1). The analog uses a three-node nozzle and three-node combustion chamber thermal representation with convective heating from the combustion gases, radiation to space, and conduction through attachments to the shield. Radiation is considered from the thrust chamber to the shield. A two-node representation of the propellant lines is assumed to connect the thrust chambers to the propellant valves. Total heat loss for the three-chamber module is shown in Fig. 11 over a thruster temperature range for the conditions noted on the curve.

A projection of the thermal response for a Tridyne thruster incorporating design refinements showed that 0.60 T_{ss} could be attained in 2 sec, 86% in 4 sec, and 99% in 8 sec. The refinements include small catalyst pellets (0.020-in.-o.d.), reduced catalyst mass (0.14 gm), thin retaining screens (0.004 in.), and minor changes to the thruster contour to permit use of thinner walls (0.0025 in.) in the chamber body. Conventional modular installation features of reflective insulation and low-conductivity inlet lines are included in the projection thermal analysis.

A weight comparison of a Tridyne system with competitive systems is shown in Fig. 12. Conventional attitude-control systems employing cold gas GN_2, heated GN_2 (Advanced Resistojet), heated propane, and a decomposed hydrazine system with a plenum chamber were synthesized from Ref. 7 system data. The general structures of the systems are shown schematically in Fig. 13. Tridyne (Fig. 13d) compares favorably with the lighter systems, retaining the simplicity of the cold gas system, which also can be represented by Fig. 13d without the catalyst or thermal control of the thrusters.

Conclusions and Recommendations

The feasibility of using Tridyne in attitude control thrusters in the 0.01-lb-thrust class has been demonstrated. Criteria are also available for catalyst optimization, thruster module designs, and efficient thruster fabrication.

The major advantage of the Tridyne concept over an inert gas is in the improved specific impulse of the reactive gas, which results in a higher over-all system efficiency. Tridyne delivered I_{sp} is 138 sec compared to 70 sec normally delivered by GN_2 systems. Additionally, the thermal insulation of a Tridyne module permits an efficient use of low-power electrical heaters to supplement the gas chemical energy, if desired.

Logical applications of Tridyne thrusters are in attitude control systems for satellites, spacecraft, and space probes. They are also ideally suited for spacecraft stabilization during inertia wheel despin operations.

Many spacecraft missions require both pulse-mode and extended-duration operation from the attitude control system. This type of operation is efficiently performed by use of reactive gases for precise impulse bits and for high-performance continuous firings.

References

[1] Barber, H. E., "Advanced Pressurization Systems Technology Program, Final Report," AFRPL-TR-66-278, Nov. 15, 1966, Rocketdyne, Canoga Park, Calif.

[2] Roberts, R. W., "Hydrogen/Oxygen Catalytic Ignition Studies for Application in the J-2 Engines," RR 64-2, Jan. 1964, Rocketdyne, Canoga Park, Calif.

[3] Roberts, R., Burge, H., and Ladacki, M., "Investigation of Catalytic Ignition of Oxygen/Hydrogen Systems," R-6303 (NAS CR-54657), Dec. 1965, Rocketdyne, Canoga Park, Calif.

[4] Falkenstein, G. et al., "Evaluation and Demonstration of the Use of Cryogenic Propellants (O_2/H_2) for Reaction Control Systems, Vol. I: Experimental Evaluations and Demonstrations," CR-72176, June 1967, NASA.

[5] Rodewald, N. et al., "Evaluation and Demonstration of the Use of Cryogenic Propellants (O_2/H_2) for Reaction Control Systems, Vol. II: Experimental Evaluations and Demonstrations," CR-72244, June 1968, NASA.

[6] *Low-Thrust Space Propulsion*, Office of the Director of Defense Research and Engineering, Washington, D. C., 1967.

[7] "Spacecraft Attitude Control Gas Systems Analysis," Final Rept. SSD70172R/JPL, Contract 951720, 1967, Space Systems Div., Hughes Aircraft Co., El Segundo, Calif.